Optimization of Inverse Laplace Transform Analysis of NMR Magnetization Data

Hyeonseon Choi

8/28/2020

We investigate the effectiveness of the Inverse Laplace Transform (ILT) analysis of NMR magnetization data in obtaining spin-lattice relaxation rate (W_1) distributions. The ILT analysis method provides an estimation of the probability distribution of W_1, which is significant in the study of condensed matter systems such as high-temperature superconductors. To observe the effectiveness of the method, we compare the probability distributions obtained for spin magnetization recovery curves of spin ½ nuclei with a stretched exponential form to analytic solutions of the distributions. For further study of the method, parameters such as the number of points and noise for the recovery curves are varied to observe their effect on the estimation of the probability distribution. We observe that these parameters contribute to unwanted oscillatory behavior in the estimated probability distribution solved using the ILT analysis method.

1. Background

1.1. Nuclear Spin

Nuclei with an odd number of protons and neutrons have an intrinsic angular momentum I or "spin", and a corresponding magnetic moment μ. These two quantities are related to each other by the gyromagnetic ratio γ, a constant specific to a nucleus' element and isotope.

$$\vec{\mu} = \gamma\vec{I} \tag{1}$$

When an external magnetic field B is applied, each nucleus in the system will possess some potential energy based on its magnetic moment's orientation in respect to the magnetic field. It is standard for the direction of the magnetic field to correspond to the z-axis.

$$U = -\vec{\mu} \cdot B\,\hat{z} \tag{2}$$

The potential energy is minimized when the direction of the magnetic moment is aligned with the direction of the magnetic field. As a result, the magnetic moments in a system will be polarized. The magnetization of a system is a vector quantity that expresses the density of the polarized magnetic moments.

When there is an angle between the net magnetic moment, the magnetization and the direction of the magnetic field, torque is generated.

$$\tau = \vec{\mu} \times B\,\hat{z} \tag{3}$$

The magnetization vector precesses around the z-axis until it relaxes back to its equilibrium position.

The angular frequency of the precession is called the Larmor frequency ω_L. Its value is dependent on the magnitude of the external magnetic field and the gyromagnetic ratio.

1.2. NMR Measurement

Nuclear Magnetic Resonance (NMR) can be used to measure the interactions between the nuclear spins and their environment in a sample.

To initiate an NMR measurement, an external magnetic field is applied to polarize the sample's nuclear spins. The nuclear magnetic moments are aligned, and the resulting magnetization vector lies on the z-axis. Then, the magnetization is rotated 90 degrees about the transverse axis by applying a radiofrequency (RF) signal that oscillates at the Larmor frequency. The magnetization vector begins to precess and generates an oscillating magnetic field that induces a voltage signal in a solenoid as it relaxes back to its equilibrium position.

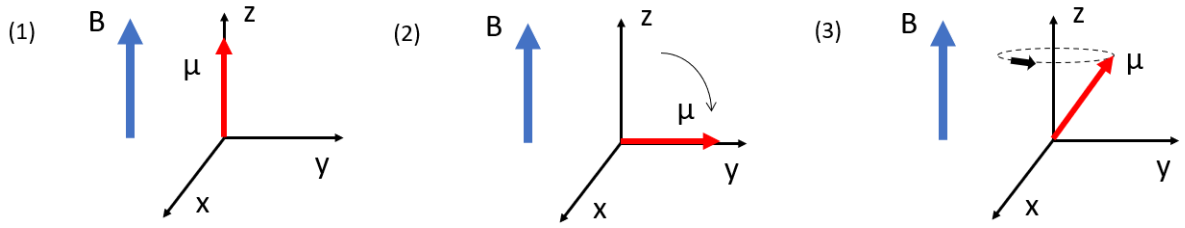

Figure 1: NMR measurement process. (1) The magnetization is aligned to the external magnetic field B. (2) Then, the magnetization is rotated onto the transverse axis by an RF signal. (3) As a result, the magnetization precesses around z-axis as it relaxes.

The voltage signal oscillates as the x-y components of the magnetization vector precess around the external magnetic field. The signal strength also decays as the z component of the magnetization vector, M_z, returns to its position parallel to the external magnetic field. This signal obtained is called the Free Induction Decay (FID) (Fig. 2).

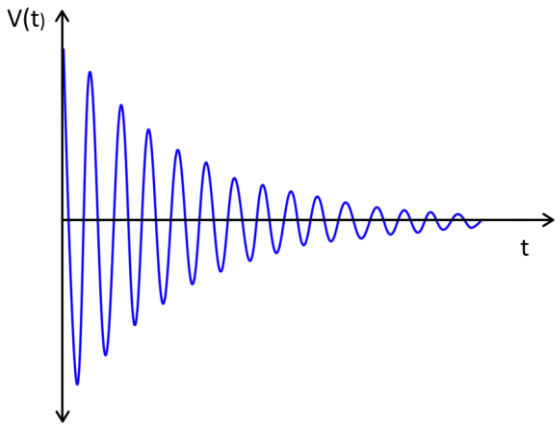

Figure 2: FID signal example: voltage induced oscillates and decays over time due to relaxation of the magnetization after perturbation.

A quantity called the spin-lattice relaxation rate (W_1) can be measured using NMR measurements. W_1 can provide insight on the interactions between nuclear spins and their environment. To measure the W_1 of a sample, an NMR measurement technique called inversion recovery is used. The technique uses a sequence of RF signals that inverts the magnetization to the z-axis, allows it to relax for a time t, and then creates a spin echo to measure the magnitude of the (partially) relaxed magnetization. The FID signals obtained from this sequence are used to measure relative M_z values during the relaxation period. The relative M_z values are plotted versus corresponding time points throughout the relaxation period to obtain a magnetization recovery curve (Fig. 3).

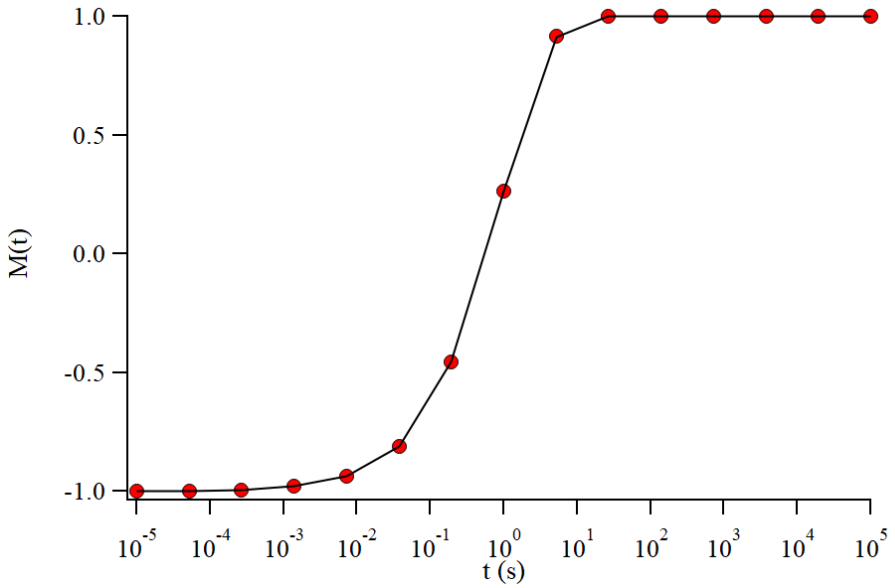

Figure 3: Example magnetization recovery curve. The curve is normalized so that when the magnetization is rotated 180 degrees from its initial position, M(t) corresponds to a value of -1. When the magnetization is back at its initial position after perturbation and relaxation, M(t) corresponds to a value of +1.

M_z relaxes exponentially according to Eq. 4 for a system of ½-spin nuclei:

$$M(t) = M_0(1 - 2e^{-W_1 t}) \quad (4)$$

By fitting the magnetization recovery curve to Eq. 4, W_1 of the system can be obtained.

1.3. Spin-Lattice Relaxation Rate (W_1)

The spin-lattice relaxation rate W_1 is the rate at which a system's magnetization's z component relaxes after it has been perturbed in an NMR measurement. W_1 corresponds to the relaxation mechanism by which the system returns to its equilibrium state by giving energy to the surrounding lattice. The value of W_1 is dependent on the interactions between nuclear spins and their surroundings. Nuclear spins can couple with nuclear spins and electron spins in their vicinity, which can affect the W_1 of the system.

A system can also be defined by a distribution of W_1 due to an inhomogeneous environment within the material. Materials can have localized regions of charge and spins that can induce various W_1. For instance, high-temperature superconductors exhibit "glassy" behavior, a type of electronic ordering. Glassy materials have electron spin fluctuations that have no preference to orientation. Such materials have a distribution of W_1 as the nuclear spins couple to these electron spin fluctuations, which are not uniform. In this case, the measured magnetization recovery no longer fits Eq. 4, a single exponential function. To study the spin dynamics of materials such as high-temperature superconductors, a distribution of W_1 needs to be considered.

1.4. Inverse Laplace Transform Analysis

The relaxation rate of nuclear spins in a sample are affected by their surroundings. There may be a distribution of various relaxation rates measured in a sample due to the inhomogeneity in the environment.

M_z recovery data is often fit to a phenomenological stretched exponential form to obtain a characteristic W_1 (W_1^*) and stretching exponent β.[1]

$$M(t) = 1 - 2e^{-(W_1^* t)^\beta} \quad (5)$$

Unfortunately, it is not necessarily straightforward to understand the microscopic origin of these phenomenological parameters. This is particularly true for higher spin nuclei (spin 3/2 or higher). To achieve an estimation of such W_1 distribution, the Inverse Laplace Transform (ILT) analysis method is used.[2,3] While the method does not use inverse Laplace transform to obtain the W_1 distribution, it is named after it due to similarities in concept and for the sake of simplicity.

M_z recovery can be expressed as an integral over W_1 values of the recovery expression and a corresponding probability with experimental noise ε_i at each point in the recovery curve. The goal is to obtain $P(W_1)$, the probability distribution of W_1.

$$M(t_i) = \int_0^\infty (1 - 2e^{-W_1 t_i})\, P(W_1)\, dW_1 + \mathcal{E}_i \quad (6)$$

The M_z recovery integral expression is similar to the Laplace transform with the function f(t) analogous to $P(W_1)$.

$$F(s) = \int_0^\infty e^{-st} f(t)\, dt \quad (7)$$

However, while the inverse Laplace transform can be applied to analytically obtain f(t), a straightforward inversion technique cannot be used to obtain $P(W_1)$ from the integral expression for M_z.

$$f(t) = L^{-1}\{F(s)\} = \frac{1}{2\pi i}\int_{-i\infty}^{i\infty} e^{st}\, F(s)\, ds \quad (8)$$

This is due to the noise measured in the experiment included in Eq. 6. When a direct inversion technique like the inverse Laplace transform is applied, the noise may be interpreted as a high frequency relaxation rate component. This may result in various solutions of the probability distribution function; the inversion is ill-posed. Rather, the probability distribution needs to be numerically estimated.

An approximation of $P(W_1)$ can be achieved using linear algebra and statistical analysis techniques. Eq. 6 can be expressed as a vector equation. The integral over the recovery expression can be expressed as a matrix called the kernel matrix. The recovery and probability distribution can be expressed as vectors. The dimensions of the vector $\vec{P}$ correspond to the number of bins set in the W_1 domain.

$$k(t_i, W_{1j}) = 1 - 2e^{-W_{1j} t_i} \quad (9)$$

$$P_j = P(W_{1j}) \quad (10)$$

$$K_{ij} P_j = \int_0^\infty k(W_{1j}, t_i)\, P(W_{1j})\, dW_1 \quad (11)$$

$$M(t_i) = K_{ij} P_j + \mathcal{E}_i \quad (12)$$

To find the vector $\vec{P}$, we minimize the quantity:

$$\phi(\vec{P}) = \frac{1}{2}\left|\widetilde{K}\,\vec{P} - \vec{M}\right|^2 + \frac{1}{2}\alpha\left|\vec{P}\right|^2 \quad (13)$$

The terms are non-negative squares as $\vec{P}$ can only be positive by definition. The non-negative constraint also serves to narrow down the possible solutions for $\vec{P}$. A best fit to the experimental data with noise is made with kernel matrix $\widetilde{K}$ and the estimated solution to $\vec{P}$. The first term is the sum of residuals squared between the fit and the experimental data. This term is minimized to achieve the best fit to the experimental data for the estimation of $P(W_1)$. The second term is the Tikhonov regularization parameter α multiplied by the squared magnitude of $\vec{P}$.[4] Estimations of $\vec{P}$ obtained by the ILT analysis method can have artificial oscillations in its distribution.[5] The oscillatory behavior increases with noise in the recovery data. The optimal α "smooths out" the

oscillations, and generally increases with greater amounts of noise. By minimizing Eq. 13, a unique estimation of $\vec{P}$ can be obtained based on experimental data with noise.

The goal of the project is to determine the effectiveness of ILT method based on experimental parameters and quantities such as the number of points and noise in the recovery curve. To study condensed matter systems such as high-temperature superconductors, accurate estimations of $P(W_1)$ must be obtained from experimental recovery data. We find the ILT method needs to be optimized to obtain such estimations.

2. Computation Method

We tested the effectiveness of the ILT method by comparing $P(W_1)$ obtained using ILT and analytic solutions of $P(W_1)$ for stretched exponential magnetization recovery curves for spin-1/2 systems (Eq. 5) (Fig. 4).

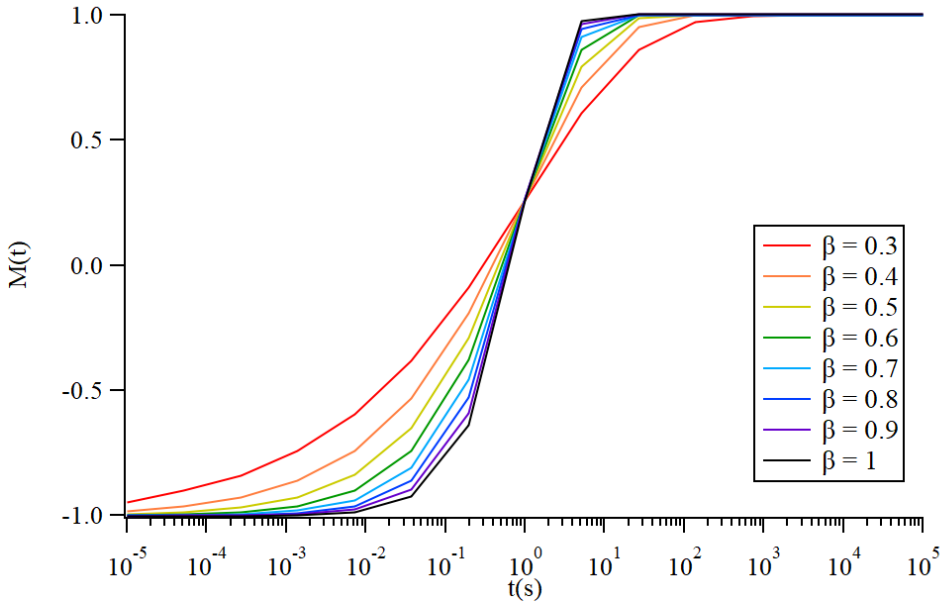

Figure 4: Stretched exponential recovery curves based on β, the stretching exponential term. β ranges from 0.3 to 1 in increments of 0.1. As β increases, the recovery curve becomes steeper.

Stretched exponential recovery functions have analytic solutions of $P(W_1)$, which were calculated using Eq. 14 and 15.[1] W_1^* is the characteristic relaxation rate, and β is the stretching exponential term. The solutions are plotted in Fig. 5.

$$s = \frac{W_1}{W_1^*} \tag{14}$$

$$P(s,\beta) = \frac{1}{\pi}\sum_{n=1}^{\infty} \frac{(-1)^{n+1}\,\Gamma(n\beta+1)}{n!\,s^{n\beta+1}}\,\sin(n\pi\beta) \tag{15}$$

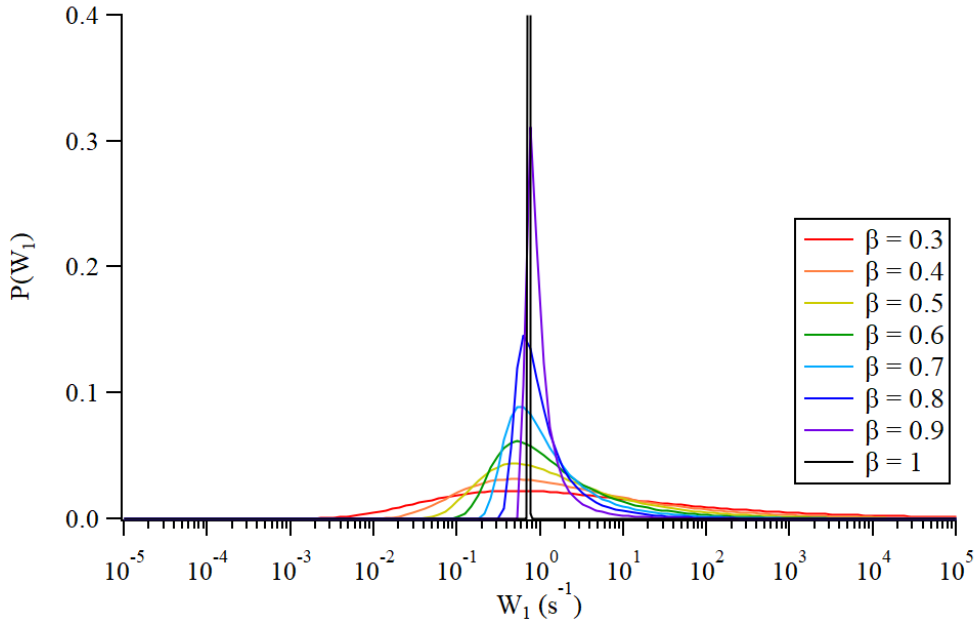

Figure 5: The analytic solutions of $P(W_1)$ of stretched exponential recovery curves made with various β, the stretching exponential term. β ranges from 0.3 to 1 in increments of 0.1. As the stretching exponential, β increases, the probability distribution becomes narrower. At β = 1, the probability distribution is a delta function.

The stretched exponential recovery curves were made by using Eq. 5. The time domain ranged from 10^{-5} to 10^{5}. The recovery points were logarithmically spaced in respect to the time. Recovery curves were made with varying experimental parameters such as the number of recovery points and noise. Their $P(W_1)$ were obtained using the ILT analysis method and were compared to the analytic solutions. The comparisons were studied to provide insight on how experimental parameters affect the performance of the ILT analysis method. Computations were performed on the software Igor Pro V8.04.

In the first round of $P(W_1)$ comparisons, stretched exponential recovery curves were made with various β, 15 recovery points, and no noise. These curves reflected data from an ideal experiment as they had no noise. 15 recovery points were chosen, because it is the standard number of points measured in experiment. In the second round of comparisons, recovery curves were made with various number of points with no noise. In the third round of comparisons, recovery curves were made with 15 recovery points and noise. Noise was added to each point based on a Gaussian distribution of some standard deviation. The standard deviations used were 0.01, 0.05, and 0.1, which correspond to signal-to-noise ratios (SNR) of 100, 20, and 10. The second and third round of comparisons were made to study the effects of experimental parameters on the ILT analysis method.

3. Results and Discussion

3.1 "Perfect Recovery Curve"

The stretched exponential recovery curves in the first round of $P(W_1)$ comparisons were made with "perfect" experimental parameters. The recovery curves were made with no noise and 15 recovery points. $P(W_1)$ of recovery curves made with select β (0.5, 0.7, 0.9) are shown in Fig. 6, 7, 8 respectively and compared to their analytic solutions.

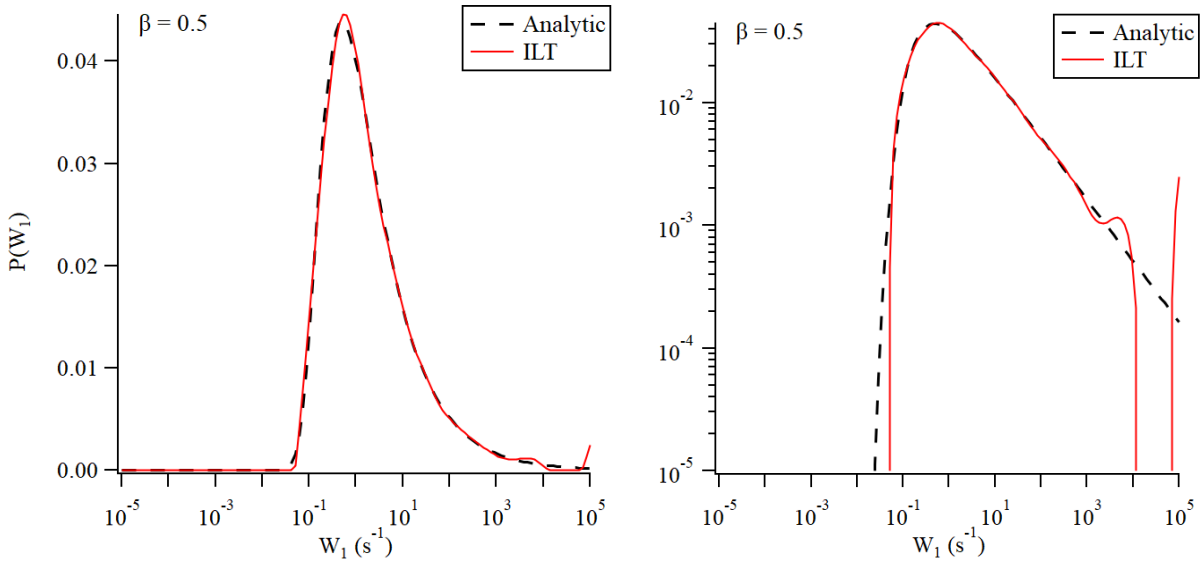

(a) (b)

Figure 6: Comparison between $P(W_1)$ obtained from ILT analysis and the analytic solution. The recovery curve was made with 15 points and no noise at β = 0.5. Figure (a) is the comparison in linear scale, and Figure (b) is the comparison in logarithmic scale.

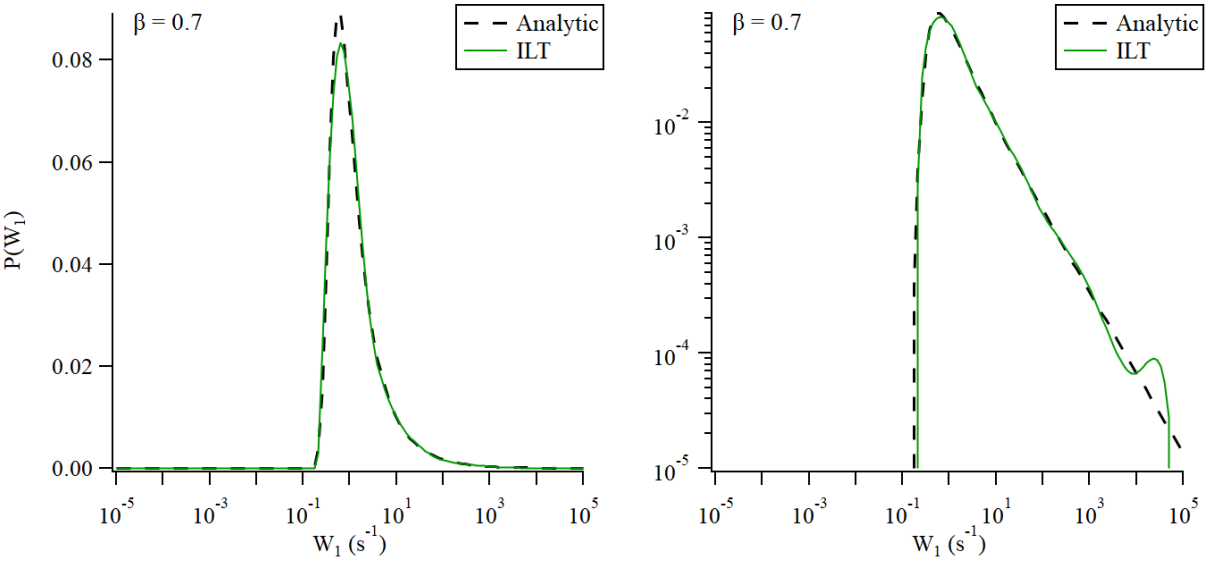

(a) (b)

Figure 7: Comparison between $P(W_1)$ obtained from ILT analysis method and the analytic solution. The recovery curve was made with 15 points and no noise at $\beta = 0.7$. Figure (a) is the comparison in linear scale, and Figure (b) is the comparison in logarithmic scale.

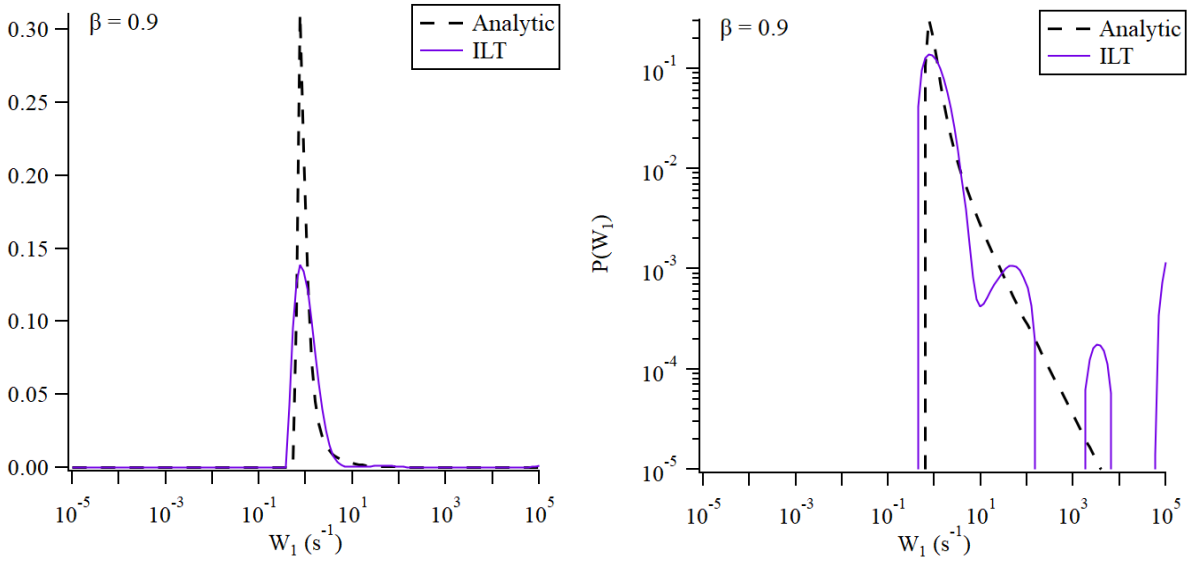

(a) (b)

Figure 8: Comparison between $P(W_1)$ obtained from ILT analysis method and the analytic solution. The recovery curve was made with 15 points and no noise at $\beta = 0.9$. Figure (a) is the comparison in linear scale, and Figure (b) is the comparison in logarithmic scale.

The ILT analysis method is more efficient at obtaining accurate $P(W_1)$ estimations for recovery curves made with smaller β. The analytic solutions for the $\beta = 0.5$ and $\beta = 0.7$ recovery curves are broader, and the estimated solution fits the analytic solution well. However, the analytic solution for the $\beta = 0.9$ recovery curve is narrower, and the estimated solution does not fit the analytic solution well. The smoothing parameter in the ILT analysis method may be excessively smoothing out the general distribution for recovery curves made with higher β. Thus, the ILT analysis method may not provide the best estimations for recovery curves that are fit to a high β.

In addition, there are artificial bumps in the $P(W_1)$ for the $\beta = 0.5$ recovery curves in the high W_1 region. This is due to the inability to capture the complete recovery of Mz in the selected time domain. For stretched exponential recovery curves made with small β, the recovery curve is "stretched", and a higher range time domain is needed to capture the entire curve. In the case of the recovery curve made with $\beta = 0.5$ (Fig. 4), there are very fast W_1 components as the selected time domain cannot capture the magnetization's starting value (-1) in the relaxation process. Thus, the $P(W_1)$ at high W_1 for the $\beta = 0.5$ recovery curve (Fig. 6) is discontinuous and

oscillatory due to the lack of information concerning the recovery curve. In experiment, it is difficult to capture the value M_z at very small times, so it may not be viable to expand the time domain outside of simulation. However, systems with recoveries fit to a stretched exponential function with $\beta < 0.7$ are rarely observed, so this issue may not need to be considered in the optimization of the ILT analysis method.

The ILT analysis method can provide accurate estimations of $P(W_1)$ for recovery curves that are fit to stretched exponential functions within a certain range of β due to concerns of excessive smoothing. Optimizations have to be made concerning the smoothing parameter α for the method to provide valid $P(W_1)$ estimations for curves fit to higher β.

3.2 Number of Recovery Points

The stretched exponential recovery curves in the second round of $P(W_1)$ comparisons were made with various number of points to study how the number of recovery points affects the P(W1) obtained from the ILT analysis method. $P(W_1)$ of recovery curves made with select number of points (8, 15, 20) and $\beta = 0.7$ are shown and compared to the analytic solution (Fig. 9).

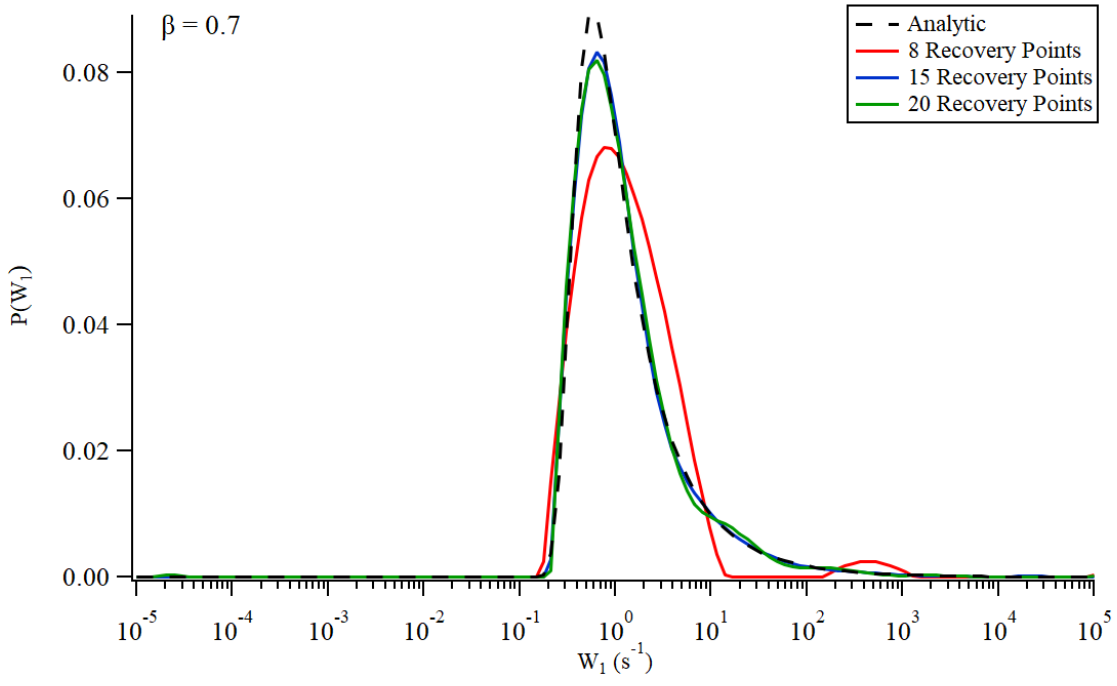

(a)

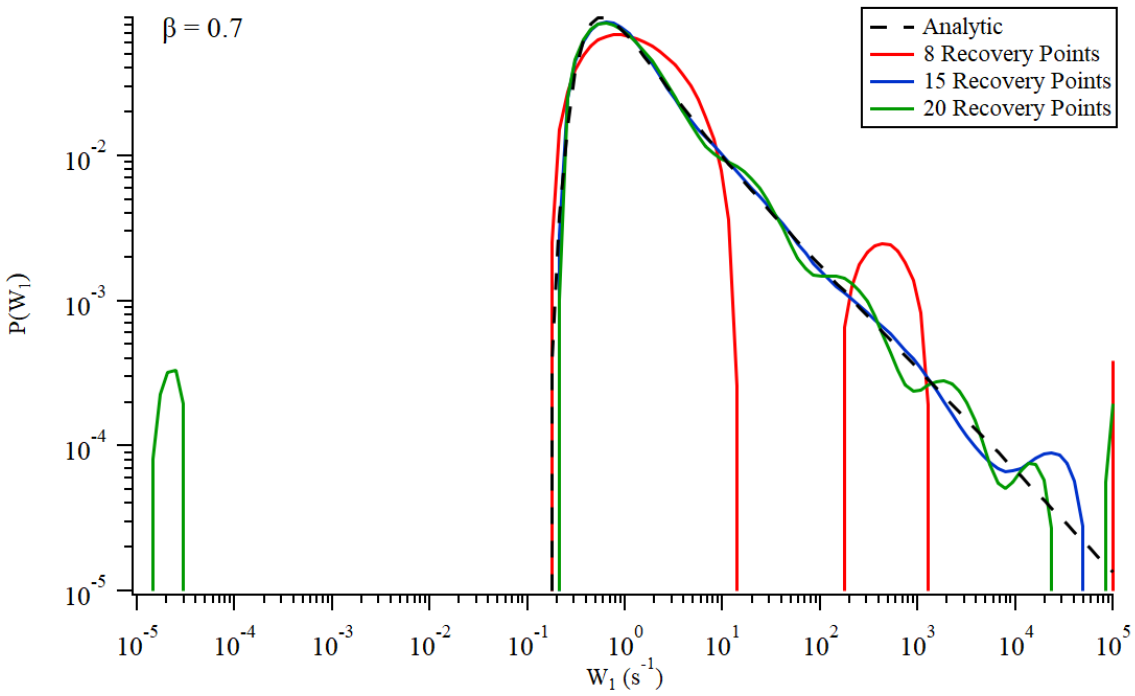

(b)

Figure 9: Comparison between $P(W_1)$ obtained from ILT analysis method for recovery curves made with 8, 15, 20 points and the analytic solution. The recovery curves were made with no noise at $\beta = 0.7$. Figure (a) is the comparison in linear scale, and Figure (b) is the comparison in logarithmic scale.

To obtain accurate $P(W_1)$ estimations using the ILT analysis method, the recovery curve needs to be made with an optimal number of points. From visual inspection of Fig. 9, it appears the number of points in the recovery curves affect the oscillatory behavior in the high frequency tails of $P(W_1)$ estimations. The oscillatory behavior in the $P(W_1)$ estimation for the 8-points recovery curve appears to be exaggerated as it has discontinuous amplitudes or bumps. In order to obtain $P(W_1)$ estimations without artificial bumps in the distribution, the recovery curve needs to have at least 15 points distribution for the chosen time domain (10^{-5}, 10^{5}) from visual inspection. To quantify this observation, the square sum of residuals between the $P(W_1)$ estimation and the analytical solution was calculated for recovery curves of made with various number of points ranging from 6 to 30. Then, the square sums of residuals for each recovery curve were plotted versus the number of recovery points (Fig. 10).

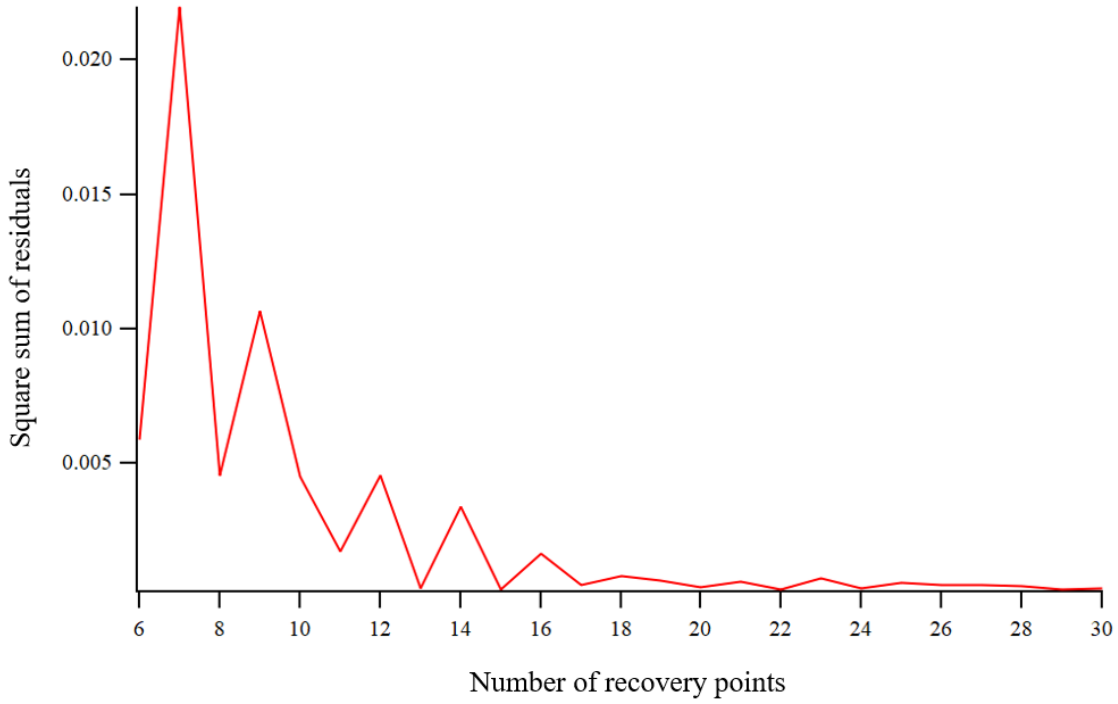

Figure 10: Square sum of residuals for recovery curves made with varying number of points versus the number of recovery points.

The square sum of residuals between the $P(W_1)$ estimation and the analytic solution decreases with the number of recovery points. The square sums of residuals near 0 for $P(W_1)$ of recovery curves made with a number of points greater than 15. In addition, there is no decreasing trend in the square sums of residuals with increasing number of points after 15 points from visual inspection of Fig. 10. Thus, for the chosen time domain of (10^{-5}, 10^{5}), at least 15 recovery points should be measured in experiment to obtain good $P(W_1)$ estimations using the ILT analysis method. This is not an absolute standard for the number of points, but it will result in a fit with a low square sum of residuals between the data and the calculated recovery curve based on the $P(W_1)$ estimations.

3.3 Noise

The stretched exponential recovery curves in the third round of $P(W_1)$ comparisons were made with noise to study how experimental noise can affect the $P(W_1)$ obtained from the ILT analysis method (Fig. 11). $P(W_1)$ of recovery curves made with SNR (100, 20, 10) are shown and compared to the analytic solution (Fig. 12).

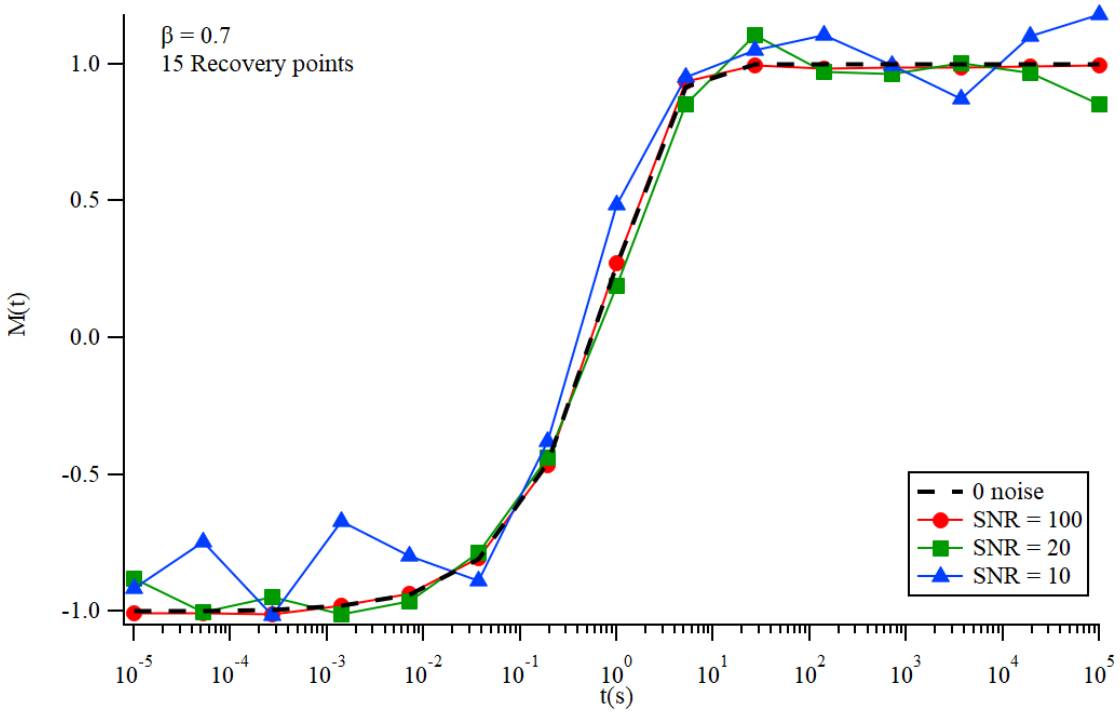

Figure 11: Stretched exponential recovery curves made with β = 0.7, 15 points, and various SNR.

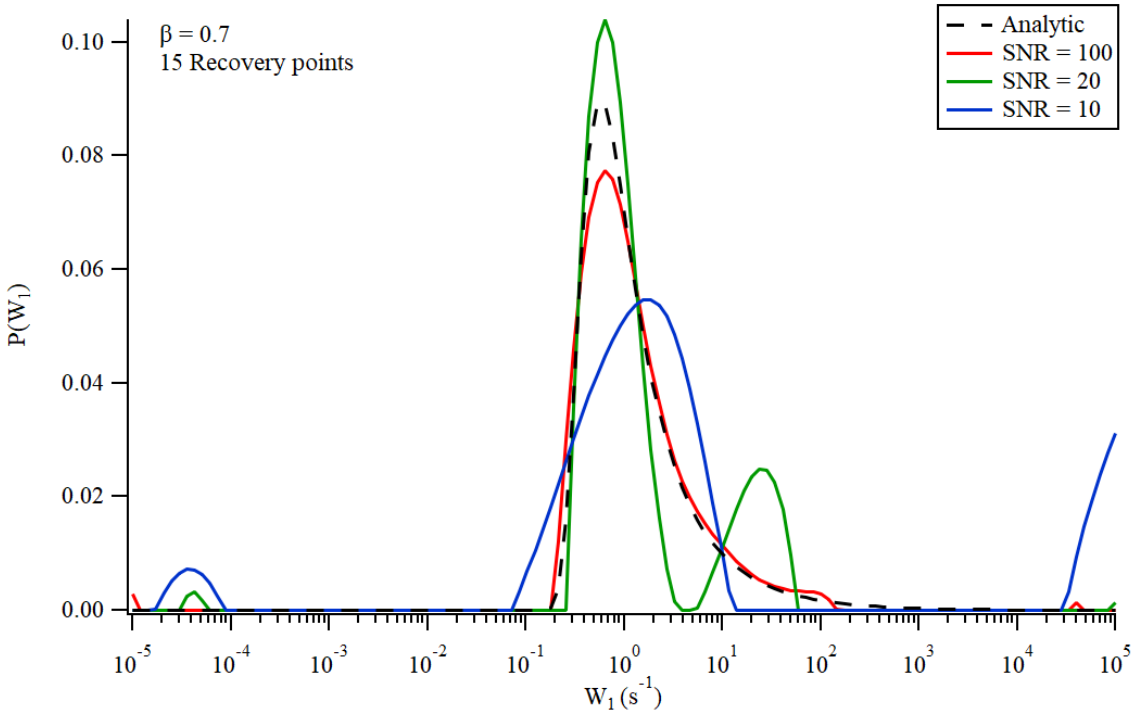

(a)

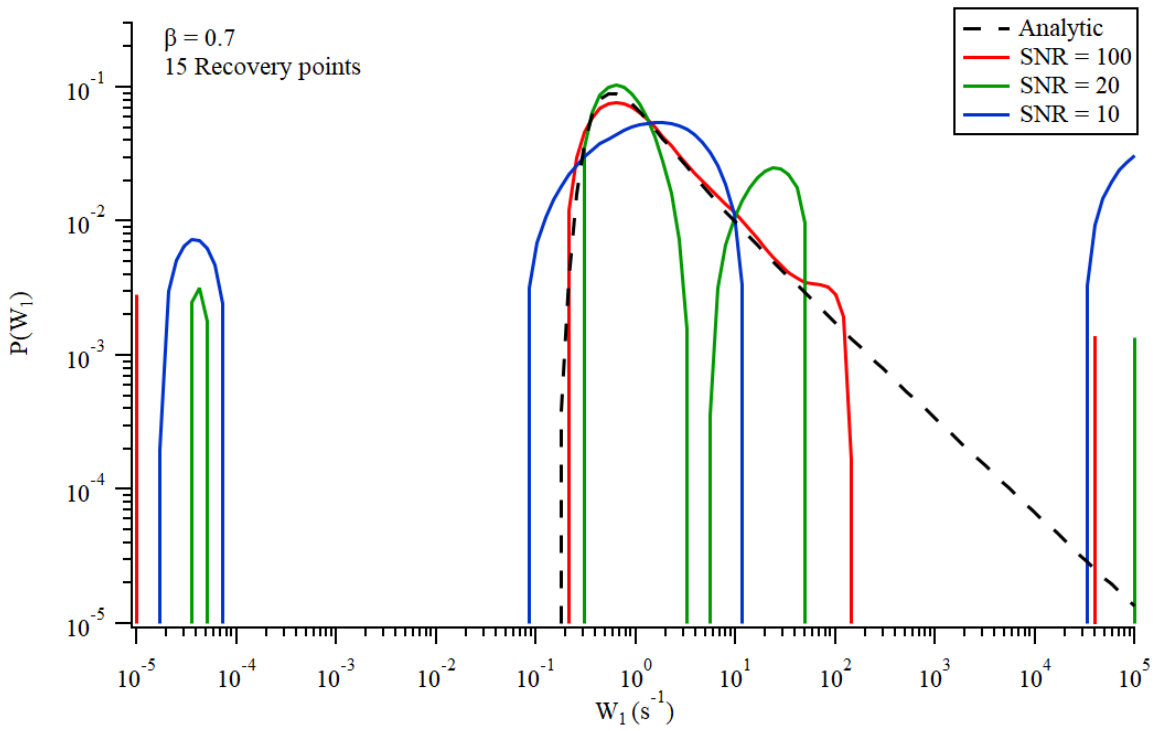

(b)

Figure 12: Comparison between $P(W_1)$ obtained from ILT analysis method for recovery curves made with varying amounts of noise and the analytic solution. The recovery curves were made with 15 recovery points at β = 0.7. Figure (a) is the comparison in linear scale, and Figure (b) is the comparison in logarithmic scale.

Noise impacts the $P(W_1)$ estimation obtained from the ILT analysis method significantly. The oscillatory behavior in the $P(W_1)$ estimations worsens with decreasing SNR as the distance between amplitudes or "bumps" increases. The smoothing parameter α cannot effectively smooth out oscillations and bumps resulting from a large amount of noise. In particular, the $P(W_1)$ estimation for the recovery data with a SNR or 10, the distribution appears to be excessively smoothed out; yet, large bumps remain.

In addition, there are small artificial bumps in the high and low frequency domains for all $P(W_1)$ estimations in Fig. 12. This is due to the noise shifting the initial and final points of the recovery curve that indicate the start and end of the recovery. Fits to the recovery curves may not have an initial point of -1 and a final point of +1 due to the noise, which can induce artificial high and low frequency components in forms of bumps in the $P(W_1)$. Constraints to the fit may need to be added to the ILT analysis method regarding the ends of the recovery curves to reduce the bumps. Overall, the ILT analysis method needs to be optimized in regard to both the fit and smoothing parameter to obtain valid $P(W_1)$ estimations from noisy recovery data.

To further study the effect of noise on $P(W_1)$ estimations obtained by the ILT analysis method, the $P(W_1)$ estimations of recovery curves made with the same SNR were compared to the analytic solution. This comparison was made to observe how the $P(W_1)$ estimations vary for recovery curves that share the same $P(W_1)$ solution and SNR. Three recovery curves were made with $\beta = 0.7$, 15 recovery points, and a SNR of 20. Their $P(W_1)$ estimations are shown in comparison to the analytic solution (Fig. 13).

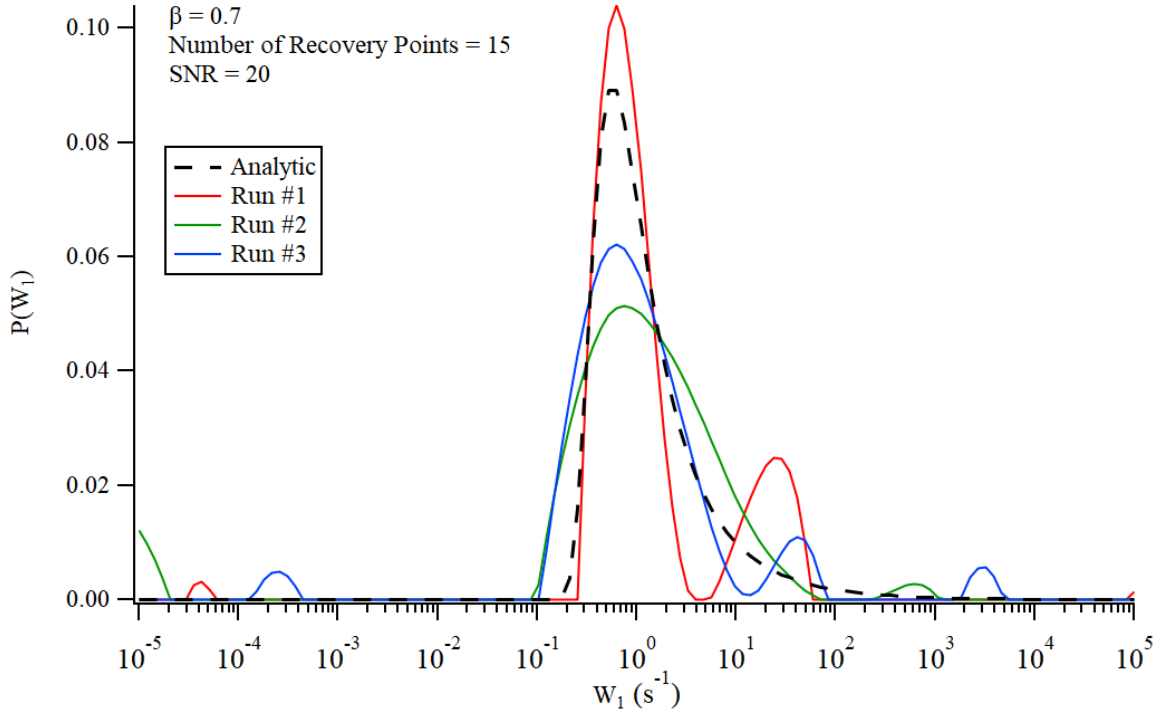

Figure 13: Comparison of $P(W_1)$ estimations of recovery curves made with $\beta = 0.7$, 15 recovery points, and a SNR of 20 and the analytic solution.

From visual inspection, the $P(W_1)$ estimations vary greatly. While the recovery curves of the estimations share the same parameters, the estimations differ significantly in aspects of peak height, oscillatory behavior, and artificial bumps. Added noise that is obtained from a Gaussian distribution with a high standard deviation has large variation. Thus, $P(W_1)$ estimations of low SNR recovery curves that share the same $P(W_1)$ solution vary greatly from each other. To quantify this, five recovery curves were made at various SNR. Their mean square sums of residuals between the $P(W_1)$ estimations and the analytic solution with error bars were plotted versus corresponding SNR values (Fig. 14).

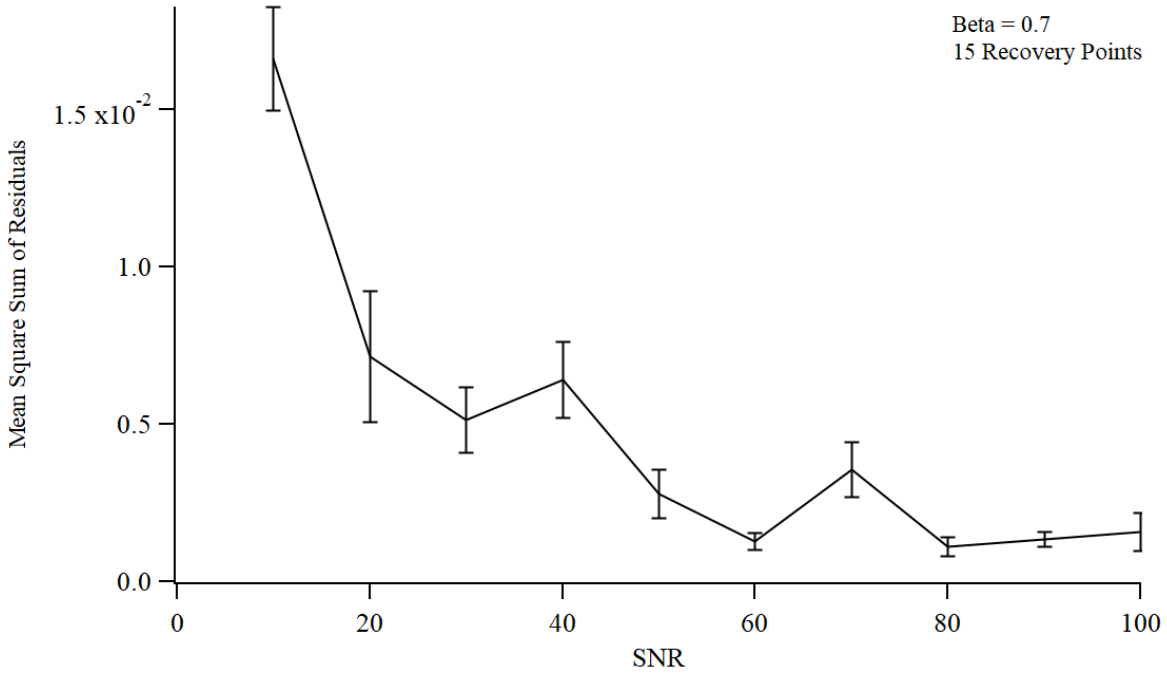

Figure 14: Mean squared sum of residuals between $P(W_1)$ estimations and the analytic solution plotted versus SNR. The recovery curves were made with $\beta = 0.7$ and 15 recovery points.

The mean squared sum of residuals and error bars generally increase with decreasing SNR. This indicates that the validity of the $P(W_1)$ estimations decreases with decreasing SNR. To obtain accurate $P(W_1)$ estimations in comparison to the analytic solution (< 5% error), experimental data with a SNR greater than 50 should be measured. Also, the large error bars indicate that many different $P(W_1)$ estimations correspond to recovery data with the same analytic solution due to the large variance in noise. Thus, it is imperative to obtain high SNR recovery data in experiment to obtain valid $P(W_1)$ estimations using the ILT analysis method.

4. Conclusion

The ILT analysis method needs optimization to obtain accurate $P(W_1)$ estimations from experimental recovery data. Experimental parameters such as the number of points and SNR can affect the oscillatory behavior in $P(W_1)$ estimations. Discontinuous oscillatory behavior occurs due to a lack of recovery points for a set time domain and a small SNR. To obtain valid $P(W_1)$ estimations with the current ILT analysis method, at least 15 points need to be obtained for the time domain of $(10^{-5}, 10^{5})$ and a SNR of at least 50 must be achieved for the experimental recovery data. However, experimental data with a SNR of at least 50 may be difficult to obtain. To obtain valid $P(W_1)$ estimations for data with lower SNRs, the smoothing mechanism in the ILT analysis method needs to be optimized. For recovery data with a lot of noise, the ILT analysis method excessively smooths out the $P(W_1)$ estimation in effort to reduce oscillatory behavior. Yet, artificial bumps still remain. Thus, an additional smoothing term or constraint

may have to be added to remedy these issues. Ultimately, the ILT analysis method is not a perfect process and can be improved upon to obtain accurate $P(W_1)$ estimations from experimental recovery data.

Acknowledgements

I would like to thank Dr. Nick Curro, Dr. Igor Vinograd, and Cameron Chaffey for their instruction and guidance throughout this project. I would also like to thank Dr. Rena Zieve and leading a great REU program.

References

[1]D. Johnston, Stretched Exponential Relaxation Arising from a Continuous Sum of Exponential Decays, Physical Review B. 74. (2013).

[2]P. M. Singer, A. Arsenault, T. Imai, M. Fujita, ^{139}La NMR investigation of the interplay between lattice, charge, and spin dynamics in the charge-ordered high- Tc cuprate $La_{1.875}Ba_{0.125}CuO_4$, Physical Review B. (2020).

[3]J. P. Butler, J. A. Reeds, S. V. Dawson, Estimating solutions of the first kind integral equations with non-negative constraints and optimal smoothing, SIAM J. Numer. Anal. 18(3), 381. (1981).

[4]A. N. Tikhonov, Regularization of incorrectly posed problems, Soviet Math. Dokl., 4, 1624-1627. (1963)

[5]D. W. Cooper, L. A. Spielman, Data inversion using nonlinear programming with physical constraints: Aerosol size distribution measurement by impactors, Atmospheric Environment 10(9), 723–729. (1976).